Computers and Concrete, Vol. 5, No. 6 (2008) 509-524
DOI: http://dx.doi.org/10.12989/cac.2008.5.6.509

Penetration resistance of steel fiber reinforced concrete containment structure to high velocity projectile

Tso-Liang Teng*

Department of Mechanical Engineering, Da-Yeh University, 112. Shan-Jiau Rd. Da-Tsuen, Changhua 515, Taiwan, R.O.C

Yi-An Chu and Bor-Cherng Shen

Chung-Shan Institute of Science and Technology, P. O. Box 90008-17-10 Lung-Tan, Tao-Yuan 325, Taiwan, R.O.C.

(Received August 16, 2006, Accepted November 5, 2008)

Abstract. Containment structures not only are leak-tight barriers, but also may be subjected to impacts caused by tornado-generated projectiles, aircraft crashes or the fragments of missile warhead. This paper presents the results of an experimental study of the impact resistance of steel fiber-reinforced concrete against 45 g projectiles at velocity around 2500 m/s. An explosively formed projectile (EFP) was designed to generate an equivalent missile fragment. The formation and velocity of EFP are measured by flash x-ray. A switch made of double-layered thin copper sheets controlled the exposure time of each flash x-ray. The influence of the fiber volume fraction on the crater diameter of concrete slab and the residual velocity of the projectile were studied. The residual velocity of the projectile decreased as the fiber volume fractions increased. In this work, the residual velocity of the projectile was to 44% that of plain concrete when the fiber volume fraction exceeded 1.5%. Based on the present finding, steel fiber reinforced concrete with the fiber volume fraction exceeding 1.5% appear to be more efficient in protection against high velocity fragment impact.

Keywords: steel fiber-reinforced concrete; high velocity impact; EFP.

1. Introduction

Nuclear power is a safe, clean and reliable source of electricity. Nuclear power plants provide around 17% of the world's electricity. However, nuclear plants are associated with some risks, many related to health and environmental effects of radioactive material. The problem of the safety of nuclear power plants has been researched in developed countries. Reactors are covered with containing reinforced concrete in an outer shell, to prevent the release of radioactive material caused by accidents. The containment structures of nuclear power plants are the final barrier between nuclear reactors and the external environment. Containment structures not only are leak-tight barriers, but also may be subjected to impacts, perhaps caused by tornado-generated projectiles, aircraft crashes or the fragments of missile warhead. The World Trade Center attacks have raised concerns about how nuclear plants should be protected from such events. Therefore, containment

* Corresponding Author, E-mail: tlteng@mail.dyu.edu.tw

structures must be designed to resists impact loads. Upgrading and strengthening plant structures and equipment is important to the future use and development of nuclear power.

The response of a concrete structure to severe loading deviates markedly from that of such a structure under a static load. When a high-velocity fragment hits a concrete wall, the wall shakes and vibrates, spalling occurs in the front, and a stress wave propagates through the concrete. This wave may cause scabbing on the reverse side of the wall. Protective structures must be designed to withstand impacts by missile fragments. Since the occurrence of the tragic events of Sep. 11, 2001 at the World Trade Center and Pentagon, there has been considerable concern among the public regarding the ability of nuclear power plants to withstand a direct attack by high-velocity projectiles. Recently studies (Ray, *et al.* 2006, Luccioni and Luege 1989) provided some methods to perform the necessity of radiological protection, structural integrity and leak tightness of containment structures, and the analysis method of the behavior of concrete pavements subjected to blast loads were recommended.

Concrete structures can effectively withstand blast waves and projectile impacts, and are commonly employed as protective structures. Adding fibers to concrete reportedly increases its toughness and impact resistance, and improves many other engineering characteristics. Various types of fibers, from natural through metallic and polymeric, are used (Mindess, *et al.* 1989, ACI Committee 1997). The use of fiber-reinforced concrete in building structures has increased because reinforcement of concrete with fibers improves its toughness, flexural strength, tensile strength and impact resistance, while favorably modifying its failure mode (Wafa and Ashour 1992, Gao, *et al*. 1997). Steel fiber-reinforced concrete (SFRC) is presently employed in sentry boxes, arms and power depots, and other defense buildings as massive armor against the impact of a projectile.

The resistance of plain and fiber-reinforced concrete against penetration and perforation by a non-deformable projectile has been studied for a long time. A review of the penetration resistance of high-strength concrete by Dancygier and Yankelevsky (Dancygier and Yankelevsky 1996) revealed scabbing at the rear face is expected to be more severe in elements that are made of high strength concrete (HSC), because of the relatively high material brittleness. A comparison of the crater dimensions in fiber-reinforced and plain concrete slab reveals that fibers tend to arrest cracks and minimize the area of damage. The experimental results of Anderson, *et al.* (1984) showed that for concrete reinforced with steel fiber with a volume fraction of up to ~3%, a larger fiber content corresponds to smaller craters, verifying the effectiveness of fibers in reducing damage caused by spalling and scabbing. A study of the impact of high-velocity projectiles on plain concrete and SFRC by Almansa and Canovas (Almansa and Canovas 1999) found that adding fiber reduced the thickness of concrete needed to prevent perforation; but the thickness necessary to avoid scabbing is much small than that for plain concrete. The results of high-velocity impact experiments on SFRC conducted by Luo, *et al.* (2000) indicated that reinforced high-strength concrete (RHSC) targets exhibited smash failure whereas SFRC targets remained intact with several radial cracks on their front faces and some minor cracks on their side faces. Another experimental investigation of the resistance of concrete, when subjected to an impact by a 12.6 mm ogive-nosed projectile, conducted by Zhang, *et al.* (2005), showed incorporation of steel fiber in the concrete reduced the crater diameters and crack propagation, but did not have a insignificantly effect on penetration depth. Dancygier, *et al*. Leppanen (2005) performed a static and dynamic penetration test of reinforced concrete (RC) slab specimens. The static tests reveal important mechanisms that govern the penetration process and therefore contribute to a better understanding of RC barriers resistance to non-deforming projectiles impact. Most of the work published so far has been based on concrete

with compressive strengths of up to 200 MPa, and impact velocities of under 1000 m/s. Increasing the impact velocity causes the penetrator front to begin to mushroom, resulting in the erosion of the penetrator, significantly degrading its penetration performance. Only limited amounts of experimental data for concrete have been reported for impact velocities of above 1000 m/s (Leppanen 2005). However, knowledge of the behavior of SFRC when subjected to higher-velocity impacts is quite limited, mainly because of the complexity of such behavior and a lack of effective methods for obtaining such knowledge.

In this work, concrete slabs that contained hook-ended steel fibers were subjected to high-velocity (above 2000 m/s) impact loading from equivalent missile fragment. The influence of the fiber volume fraction on the crater diameter of concrete slab and the residual velocity of the projectile were studied. The slab specimens had an area of 50 cm×50 cm and were 10 cm thick. High-velocity impact was caused using explosive acceleration technology. An explosively formed projectile (EFP) was designed as a high-velocity projectile generator (HVPG) device for use in a field test as an equivalent missile fragment. This work presents the results of an experimental study of the impact resistance of steel fiber-reinforced concrete with a compressive strength of 24~32 MPa and a fiber volume fraction of 0~2%, under an impact from a 45 g projectile at a velocity of around 2500 m/s. The residual velocity of the projectile and the crater dimensions were measured after the concrete slab had been shot. The effects of the fiber volume fraction on the failure behavior, the crater dimension of the concrete slab and the resistance to penetration were also studied. The results presented herein are very useful for designing containment structures to resist high-velocity projectiles.

2. High-velocity projectile generator

2.1. EFP Configuration

Since World War II, shaped charge technology has been widely used in anti-armor, anti-ship and anti-fortification warheads. The slugs of shaped charges are of two types - jets as conical charges and pellets as explosively formed projectiles (EFP). Fig. 1 displays the basic components of a shaped charge device. The device comprises an initiator or a detonator, a booster and an explosive charge encased in a charge body with a plate at one end and a hollow-cone liner at the other end. An EFP is also called an explosively formed penetrator, a self-forging fragment, a Misznay-Schardin charge, a mass focus device or a P-charge (Lloyd 1998). It is similar to a shaped charge, except in that the liner is saucer-shaped rather than conical. An EFP consists of a metallic liner, a metallic case, an explosive section and an initiator. Very often, a retaining ring holds the liner-explosive subassembly in place. Fig. 2 schematically depicts high-velocity projectile generator (HVPG) devices. Explosives such as Composition B, Octol, RDX, HMX and PBX are used because they have high detonation velocities. After ignition, the explosive generates enormous pressures that collapse the entire liner into a single high-velocity projectile, typically moving at 2~3 km/s.

2.2. Design parameters

The design of explosively formed projectile devices is determined by several parameters, which affect their characteristics and performance. Material properties of the explosive, the liner and the

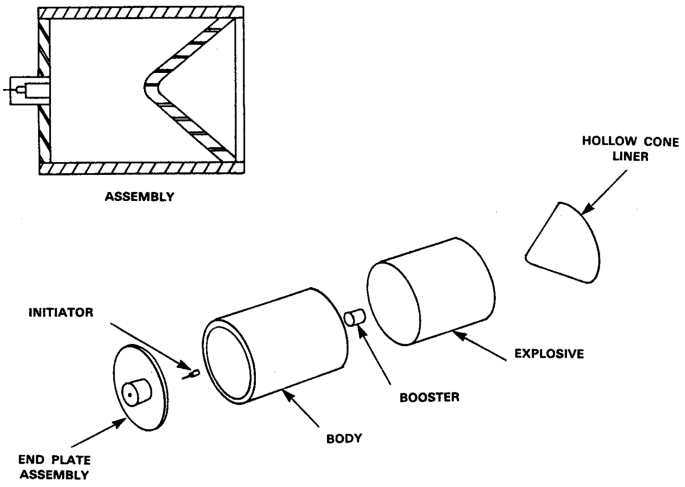

Fig. 1 Typical shaped charge device (Zukas and Walters 1998)

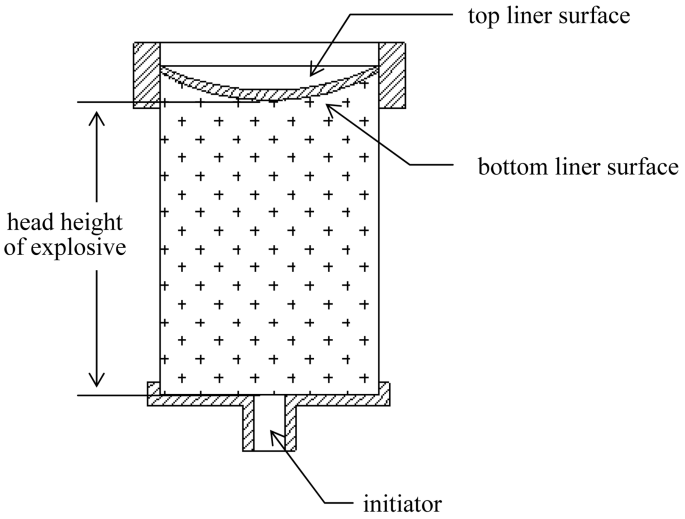

Fig. 2 Schematic diagram of high velocity projectile generator

casing are important to the design of an EFP. Other parameters are geometric, including the liner contours, the casing dimensions and the charge diameter, among others. EFP design is successful when the EFP can defeat a specific structure. Four parameters dominate the design of an EFP. They are the head height of the explosive, the thickness of the liner at its center, the profile of the top liner surface and the profile of the bottom liner surface. These parameters fall into two groups - explosive-related and liner-related.

The length of the explosive between the center point of the bottom liner surface and the bottom of the explosive is called the head height of the explosive, as shown in Fig. 2. The EFP must have sufficient explosive energy to collapse the liner. The head height should be sufficiently large to form a high-pressure wave that acts on the liner and forges it into a high-velocity projectile. If the head height is too small, then the liner may not collapse into the desired pellet or the velocity

of the pellet may be too low. Increasing the head height above around 1.5 times the charge diameter typically does very little to improve the penetration capability of a shaped charge (Walters and Zukas 1989). The head height or charge length should generally be kept to a minimum to reduce the length of the device and reduce mass. The explosive of an EFP can typically be cased and pressed. In either case, care must be taken to maintain the uniformity of the density and the distribution of the particles. Also, the grain size of the particles in the explosive may have to be controlled.

On the other hand, the material's ductility, strength and processing will influence the formation of EFP also. Copper or iron liners were typically used for of their ductility. The geometry of the bottom surface mainly influences the velocity of the liner, as a function of the curvature, in the early stage of formation. Altering the geometry of the top surface of the liner relative to the bottom surface changes the mass distribution and strength of the liner across its radius, affecting the probability that the liner breaks into many pieces in the early stage, as well as the shape of the liner in the late stage of formation. In general, more than two curvatures are used for the liner's top surface.

Finally, a tight contact must be ensured between the explosive and the liner, and symmetry also must be maintained to inhibit discontinuous wave propagation and asymmetric explosive impulses. In this work, the liner of HVPG was made of iron with a mass of 45 g, and the diameter of the liner was 57.2 mm. The liner was large enough to yield easily measurable test data and also small enough to meet the requirements of total weight of explosive in the test filed. The explosive was cast Octol 75/25. The head height of the charge was 76.2 mm. The assembled HVPG device was as presented in Fig. 3, and the mass of HVPG was 594 g.

2.3. Measurement of projectile velocity

Four high-velocity projectile generator devices (named as HVPG-1~4) were prepared and tested to

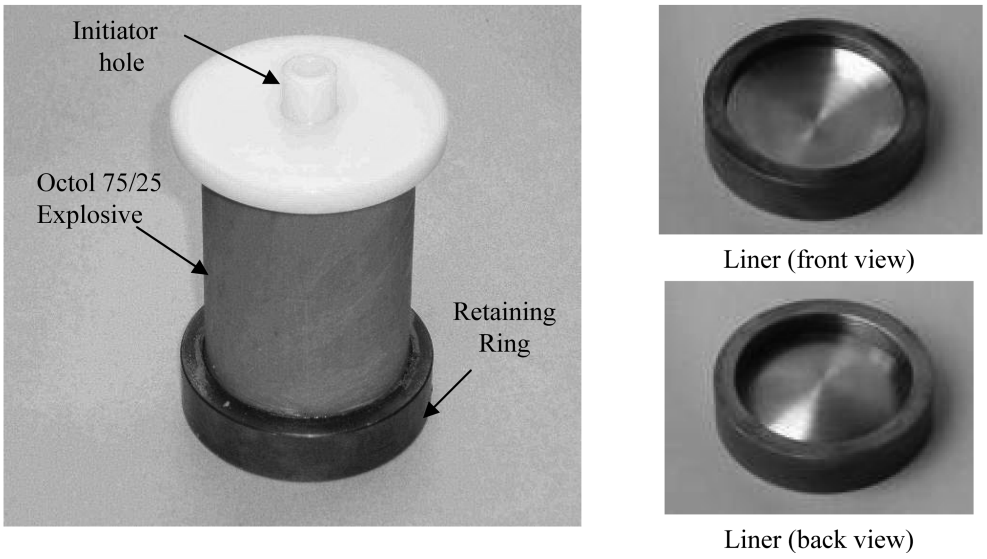

Fig. 3 Assembled HVPG device

determine the velocity and the configuration of EFPs. A two-channels flash X-ray system was employed to capture the configuration of the forming projectile at flight distances of 330 mm and 930 mm in front of the edge of HVPG device. Two radiographs of area 430×350 mm were used to display the image of the projectile and evaluate the impact velocity of the projectile. The exposure times of two flash X-ray were estimated by LS-DYNA3D finite element analysis first, in order to capture the images of formed EFP. Fig. 4 displays the radiographs from the HVPG-1 test. The exposure times of two radiographs were 151.1 μs and 391.1 μs after detonation. The two radiographs indicate that the explosively formed projectile had a semi-ellipsoid and compacted shape. The magnification ratio of the image in the film and the flying distance between the two images yields an average velocity of the projectile of 2496 m/s. The profile of EFP in x-ray film was obtained using a digitizer and then regenerated using ANSYS code to calculate the volume and mass of the projectile. The diameter and length of the projectile were 27 mm and 23 mm, respectively. Table 1 presents the test results. Fig. 5 shows the EFP profile of the remaining tests. The HVPG used in this work reliability generates an equivalent high velocity missile fragment for impact testing.

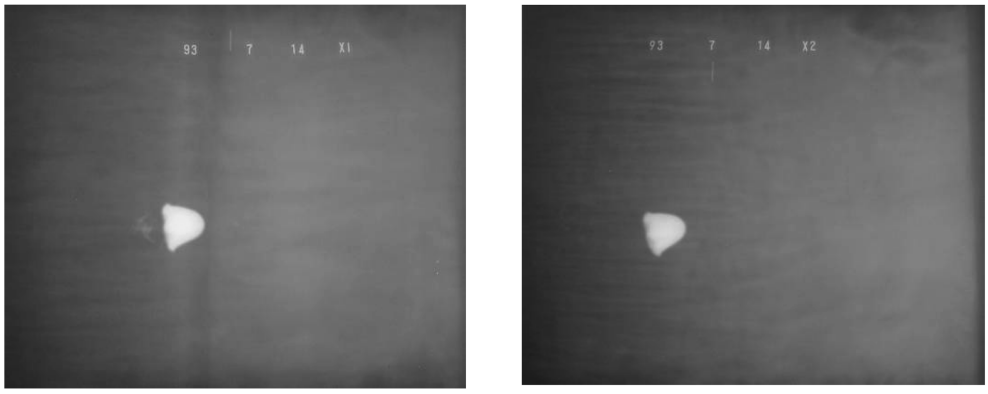

(Film #1) (Film #2)

Fig. 4 X-ray images of EFP profile of HVPG-1

Table 1 Velocity of EFP generated by high velocity projectile generator (HVPG)

Test No.	Assembled Weight (g)	X-ray exposure time (μs)		Flying Distance (cm)	Explosively Formed Projectile		
		film #1	film #2		Volume* (cm^3)	Mass (g)	Average velocity (m/s)
HVPG-1	595	151.1	391.1	59.9	5.58	43.9	2496
HVPG-2	593	151.0	391.2	59.2	5.60	44.1	2465
HVPG-3	592	151.1	391.1	59.8	5.59	43.9	2492
HVPG-4	594	151.0	391.1	58.6	5.55	43.7	2441
Average					5.58	43.9	2474

*Depicted the profile of projectile in the x-ray film and calculated by the ANSYS codes

3. Experiment and setup

3.1. SFRC specimens

The SFRC specimens were produced by a fluidized mortar and steel fiber. The manufacturing process combined mortar infiltration and vibration. Portland cement from Tashi, Taoyuan in Taiwan was employed with a maximum coarse aggregate size of 25 mm of crushed siliceous stone. Hook-ended steel fibers of length 30 mm and diameter 0.5 mm, yielding an aspect ratio of 60, were used in this work. Five concrete mixtures were formulated to evaluate the resistance of SFRC, with various fiber volume fractions, to penetration. The fiber content, v_f was 0%, 0.5%, 1.0%, 1.5% and 2.0% of the volume of concrete and added manually with care taken during mixing to prevent balling of the fibers. A vibrator was utilized to ensure proper compaction. Concrete without fibers exhibited a compressive strength of 24 MPa after 28 days. All the specimens that were subjected to impact had a size of 500 mm×500 mm and a thickness of 100 mm. Two specimens of each mixture were impact-tested. The slabs were demolded after 24 hours and cured in water for 28 days, as shown in Fig. 6, and then air-dried in the test field until testing. The compressive strength and the

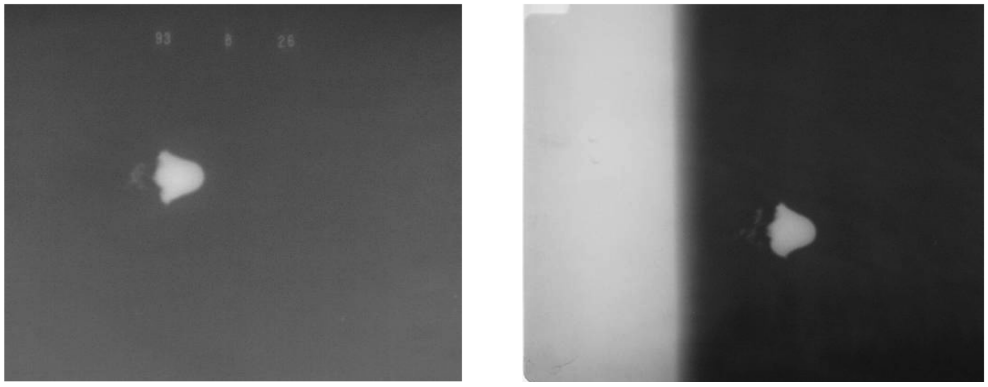

Fig. 5 X-ray images of EFP profile of HVPG-2 and HVPG-3

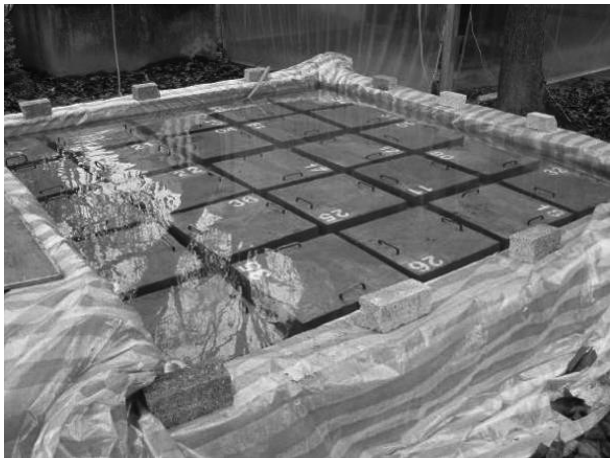

Fig. 6 Steel fibers reinforced concrete specimens

splitting tensile strength of concrete were obtained from eight 100 mm×200 mm cylinder specimens and the average material strength for each mixture was as presented in Table 2. The material test results revealed that the compressive strength and the tensile strength of concrete increased linearly with the fiber volume fraction.

Table 2 Properties of the SFRC targets

Specimen No.	Steel Fiber volume fraction (%)	Weight (kg)	Ave. Compressive Strength (MPa)	Ave. Tensile Strength (MPa)
FCA-10	2.0	64.33	31.5	5.02
FCA-10-1	2.0	63.25		
FCB-10	1.5	65.40	30.1	4.01
FCB-10-1	1.5	64.65		
FCC-10	1.0	62.24	27.7	3.60
FCC-10-1	1.0	62.35		
FCD-10	0.5	61.62	25.6	3.07
FCD-10-1	0.5	61.84		
PC-10	0.0	59.22	23.6	2.38
PC-10-1	0.0	60.31		

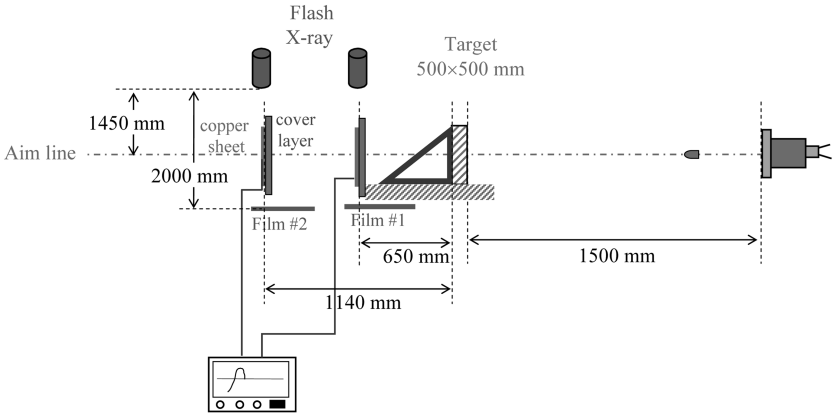

(a) schematic diagram

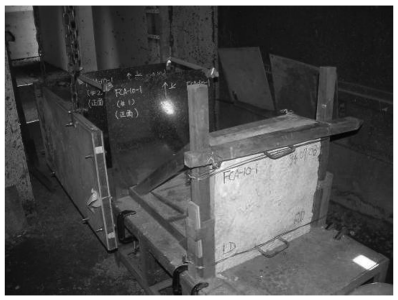

(b) front view

(c) back view

Fig. 7 High velocity impact test set-up

3.2. Experimental setup

Fig. 7 presents the experimental arrangement for the high-velocity fragment impact test. The SFRC slabs were placed on a stationary stiff steel frame on the ground as a target base. Each test specimen was placed in a triangular steel containment jig above the base to prevent motion in any direction during the impact. It was aligned such that the projectile would hit the center of the specimen. The center of plate was located 670 mm above the ground, which was the height of flash X-ray tube. Two specimens were used in the test of each concrete mixture and the average of the results thus obtained was determined. All slabs were subjected to a single impact by a semi-ellipsoid EFP of mass close 45 g with a velocity of around 2500 m/s. After it had taken an impact by the projectile, the slab was examined visually; photographs were taken, and the dimensions of the craters and cavities on both side of the slab were recorded.

The residual velocity can be obtained from the image captured by the high-speed camera or other optical device. In this experiment, the projectile may have been covered by flying concrete debris after the impact, so residual velocities might then have been measured incorrectly based on the flying concrete fragment observed by the high-speed camera. Additionally, the high explosive blast and shrapnel after detonation may damage the camera. Therefore, flash X-ray equipment was used instead, to capture an image of the remnant projectile after it had perforated the slab. Two-channels flash X-ray system was used to image the remnant projectile after it had perforated the target, to analyze the damage and measure the residual velocity. The residual velocity of the remnant projectile is unknown, so estimating the exposure time for each channel of the flash X-ray is difficult. This work proposes a switch for controlling the exposure of the flash X-ray. The switch comprises a pair of thin copper sheets separated by a thin transparent layer, which is connected to the circuit loop of the flash X-ray. When the remnant projectile simultaneously penetrates the double-layered thin copper sheets, the circuit loop is closed and the flash X-ray is triggered.

The exposure time of the flash X-ray for each channel is recorded by using a transient recorder. Two pairs of double-layered thin copper sheets were placed 650 mm and 1140 mm behind the target, respectively. The flash X-ray tubes were mounted 1450 mm from the centerline of target, and the film plane was 550 mm in reverse direction, as shown in Fig. 7. A steel plate with an area of 600×600 mm and a thickness of 1 mm was placed in front of the copper sheets as a cover plate to prevent breakage of the sheet by debris from the concrete slab, and was responsible for inaccuracies in the residual velocity of the projectile. Relating the time interval between the two exposures of the flash X-ray enables the residual velocity of the projectile to be determined from its images in two radiographs and the distance between the two switches made by double-layered thin copper sheets.

4. Experimental results and discussion

After it had received an impact from an EFP, the panel specimens were investigated visually. The resistance of SFRC to penetration by a high-velocity projectile in this work was evaluated from the crater diameter and the diameter of the cavity in both sides of the slab and the residual velocity of the projectile. The state of perforation limit was not defined; rather, the residual velocity of the projectile was measured and the penetration resistance was regressed.

4.1. Failure mode and crack behavior of specimens

The failure of a plain concrete slab (PC-10 specimen) under impact was catastrophic, as shown in Fig. 8. The projectile perforated the slab with the formation of an irregularly shaped fracture zone. It broken into many pieces but was restrained in the transverse direction by the fixed steel frame. No fine radial crack was observed on either the front or the rear side, and brittle failure occurred. The failure of the plain concrete without reinforcing fibers was brittle and the cracks extended beyond the crater region and split the specimen into pieces. Therefore, when failure conditions were present, larger craters were formed, with larger segments of the concrete separated from the plate.

Fig. 8 Failure pattern of plain concrete slabs

Table 3 Test results of high velocity fragment impact on the SFRC targets

Specimen No.	Steel Fiber content (%)	Projectile Impact Velocity (m/s)	Front Face Damage		Rear Face Damage		Projectile Residual Velocity (m/s)
			Crater diameter (cm)	Cavity diameter (cm)	Crater diameter (cm)	Cavity diameter (cm)	
FCA-10	2.0	2474[a]	32.6	17.6	32.9	19.0	–
FCA-10-1	2.0		32.8	16.9	32.4	17.6	165[b]
FCB-10	1.5		32.2	20.3	34.1	19.6	200
FCB-10-1	1.5		33.2	20.6	32.9	20.4	262
FCC-10	1.0		33.6	23.3	33.6	23.3	–
FCC-10-1	1.0		36.6	22.4	35.1	23.8	379
FCD-10	0.5		36.6	23.7	36.8	25.3	394
FCD-10-1	0.5		36.1	23.7	38.9	25.5	390
PC-10	0.0		38.4	27.5	41.4	31.0	525
PC-10-1	0.0		40.9	31.8	41.8	32.6	–

[a]Average velocity of explosively formed projectile in Table 1
[b]Predicted according to the cavity diameter in the rear face of target

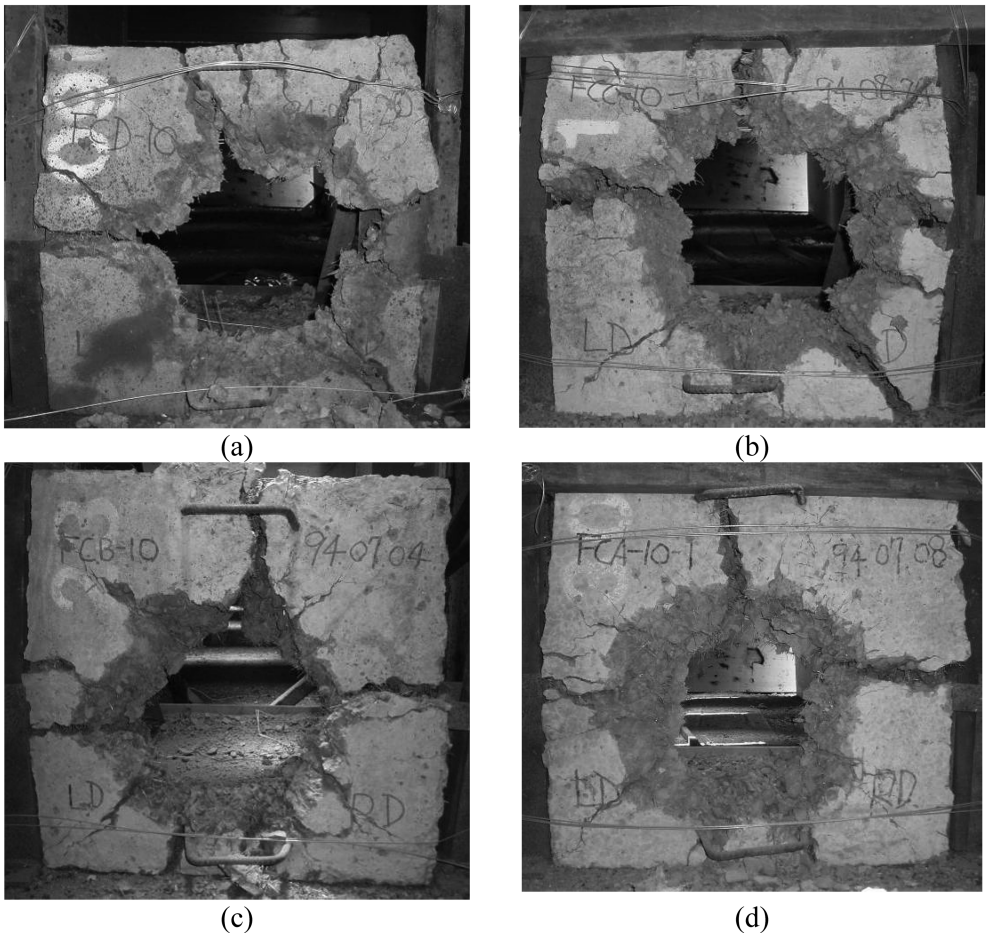

Fig. 9 Failure pattern of SFRC slab (a) 0.5% (b) 1.0% (c) 1.5% (d) 2.0%

Table 3 presents the test results of a high-velocity impact on SFRC. The crater and cavity diameters of the target were measured using a digitizer to yield the areas. The equivalent diameters were then obtained. The crater and cavity diameters in the rear face of the PC-10 slab were 41.4 cm and 31 cm, respectively.

When the volume fraction of the reinforced fibers was 0.5%, the SFRC slab (FCD-10 specimen) was perforated by the projectile, and the slab was broken into pieces with few fine radial cracks while maintaining its integrity after impact, as shown in Fig. 9. The slab failed by the formation of a shear plug and a radial crack. No regularly shaped crater was formed, which is probably related to the effect of brittle damage transfer into flexure damage on the slab with few steel fibers. The crater and cavity diameters on the rear face of the FCD-10 slab were 36.8 cm and 25.3 cm, respectively. The cavity diameter was 82% of the plain concrete. Clearly, the cavity diameter is smaller than that of plain concrete. The incorporation of steel fibers in concrete reduced the crack propagation, scabbing area and provide better resistance capability for high velocity impact.

As the volume fraction was increased from 1.0% through 1.5% to 2.0%, the SFRC slabs were still perforated by the projectile and broken into a few pieces, but the size of the shear plug and the

diameter of the cavity decreased. The number and widths of the cracks in the front and rear surfaces of the slab after the impact were reduced, and more fine radial cracks were formed, as the volume fraction increased. The damage behavior of 2.0% fibers slab (FCA-10-1 specimen) shows that only a few cracks were present in both the front and the rear sides of the slab. Similar phenomena were found in the transverse direction. Additionally, the craters in the specimen were more symmetric and almost circular-shape when the fiber volume fraction exceeded 1.5%; they had sharp edges and were asymmetrical when the fiber volume fraction was under 1.5%. The FCA-10-1 specimen (2%) had more fine radial cracks around the crater after impact, and exhibited reduced crack propagation outside the crater region, so damage was confined to a local area. The crater and cavity diameters in

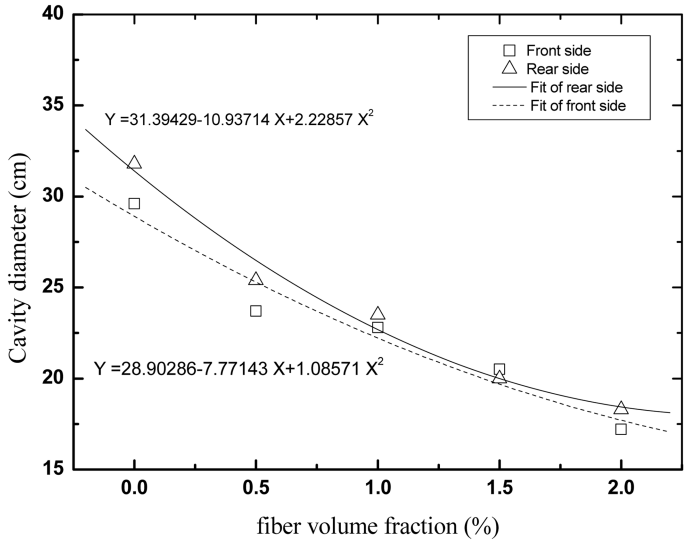

Fig. 10 Relationship between fiber volume fraction and the cavity diameter of concrete

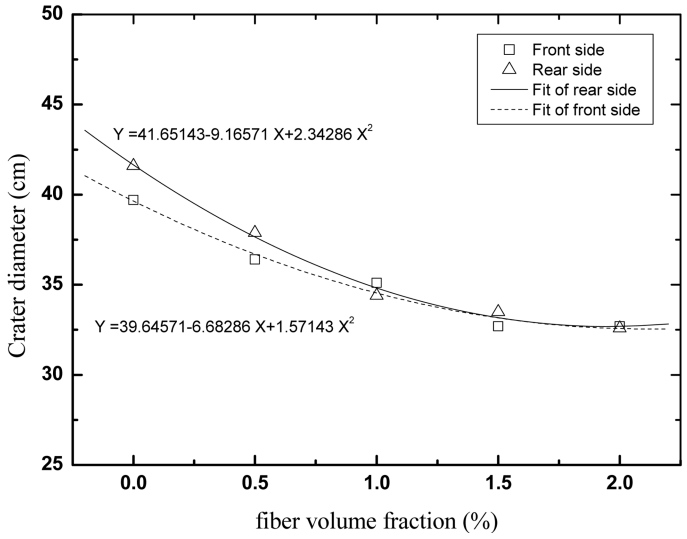

Fig. 11 Relationship between fiber volume fraction and the crater diameter of concrete

the rear face of the FCA-10-1 slab were 32.4 cm and 17.6 cm, respectively, which values are 78% and 57% of those of plain concrete, respectively. Fig. 9 shows that the steel fibers localized the damage by reducing the brittleness of the concrete, increasing the resistance to against the impact by projectile.

Fibers are spread throughout the thickness of the element, so the reinforcement of the steel fibers in the concrete matrix can increase its resistance and minimize damage both in the front and the rear faces of the slab. Comparing the dimensions of the front and the rear craters for the various mixtures indicates that increasing the volume of steel fibers inhibited the development of cracks and minimized the area of damage. Fig. 10 shows that the diameter of the cavities in both the front and the rear surfaces of the specimen decreased as the volume fraction of the fibers was increased from 0.5% to 2.0%. Fig. 11 plots a similar relationship between the crater diameter and the volume fraction of the steel fiber.

4.2. Residual velocity of projectile

The penetration resistance of high-velocity projectile impact in this work was evaluated based on the residual velocity of the projectile. The residual velocity is very important to designing and constructing protective structures, such as used at military bases and other civilian structures. It also serves as a baseline for the development of future approaches of penetration resistance.

The location of X-ray films behind the EFP aim line. Hence, after the magnification ratio of the image in the film was calculated, and the distance flown between the two images yields the residual velocity of the projectile, as given in Table 3. Fig. 12 displays the images of the projectile after the FCD-10-1 specimen (0.5%) was perforated. In film #1, the projectile was ruptured and separated into a few pieces by discrete steel fibers after impact, and no concrete debris was observed in front of the first piece of the projectile. Therefore, the projectile perforated the target in this test and successfully triggered the first channel of the flash X-ray at time of 2384 μs after detonation. In film #2, only the remnant high-energy projectile was imaged, and no scrap of concrete was observed in front of the first piece of the projectile, even when the scraps perforated the first layer. The first piece of the EFP slug perforated the cover layer and successfully triggered the second

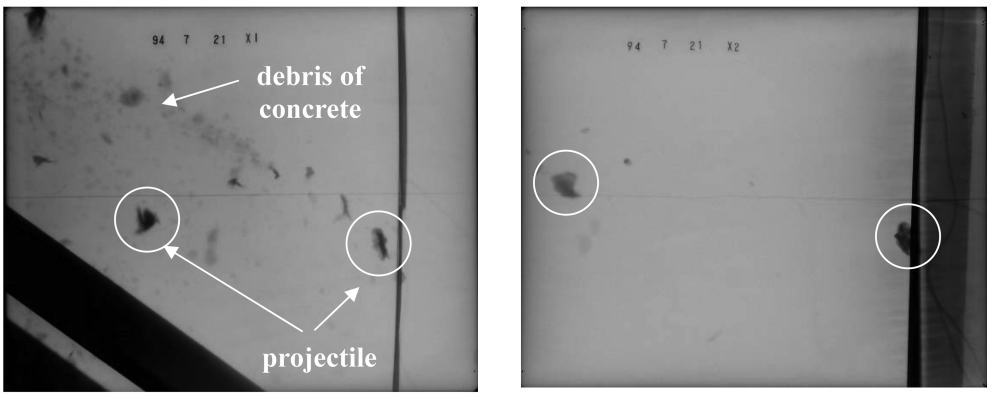

(Film #1) (Film #2)

Fig. 12 X-ray images of fractured projectile after perforated the concrete slab (FCD-10-1 specimen, V_f=0.5%)

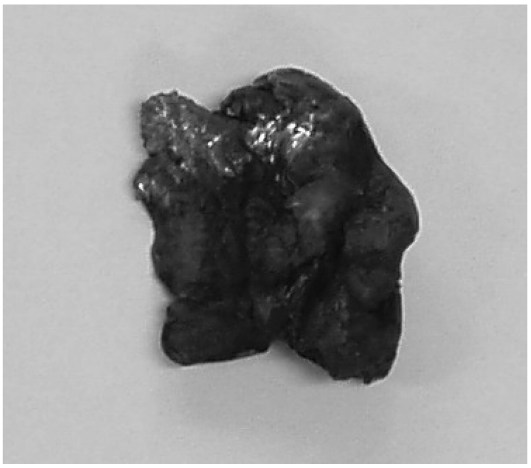

Fig. 13 The remnant projectile in the test of FCD-10-1 test

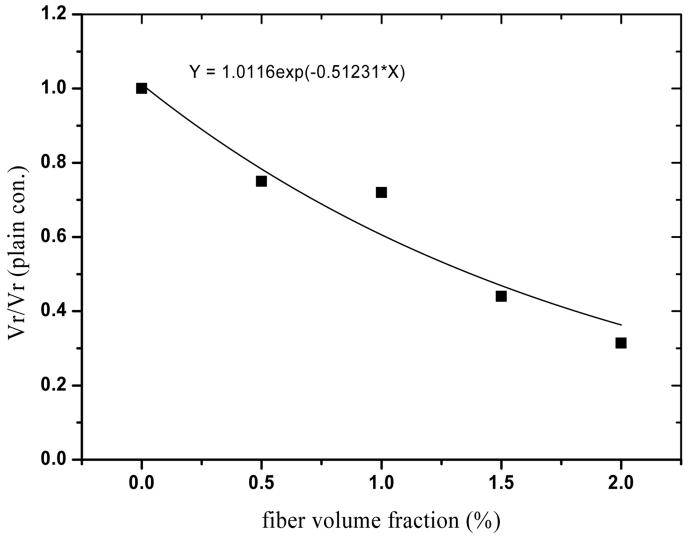

Fig. 14 Relationship between fiber volume fraction and the residual velocity of projectile

channel of the flash X-ray at time of 4062 μs. After review the x-ray images, no more debris of concrete were found in 2nd x-ray film. The remnant projectile in the test of FCD-10-1 was found after test, as shown in Fig. 13. The weight of the remnant projectile was 7.88 g. After review the residual velocity by THOR formula (Ballistic 1961), there was 10% velocity loss when perforated the aluminum plate with 1 mm thickness. Cover layer in this experiment provide sufficient resistance to penetration by the debris of the concrete slab and the steel fibers, it also minimized the energy lose of remnant EFP and prevented an incorrect determination of the residual velocity of the projectile. In FCD-10-1 test, the magnification ratio of the image in the film to the distance traveled between the two images yields the residual velocity of projectile at around 390 m/s.

Fig. 14 presents the residual velocity distribution of each mixture. As the volume fraction was increased from 0.5% to 1.0% and 1.5%, the resistance to perforation by the projectile was

improved. The residual velocity of the projectile declined as the fiber volume fraction increased in that range. However, this relationship was not linear. The test results indicate that the residual velocity of the projectile dropped to 44% that associated with plain concrete when the fiber volume fraction exceeded 1.5%, indicating that adding steel fibers into regular-strength concrete does not only markedly increase resistance to visible damage around the penetration crater, but also increases the penetration resistance by reducing the residual velocity of a missile fragment that has an impact at a velocity of around 2500 m/s.

5. Conclusions

The penetration resistance of steel fiber-reinforced concrete (SFRC) in this work was evaluated by high-velocity impact. Hook-ended steel fibers of length 30 mm and diameter 0.5 mm were used. The SFRC plates contain a maximum coarse aggregate size of 25 mm of crushed siliceous stone and the compressive strengths ranging from 23.6 to 31.5 MPa. The SFRC targets were impact and penetration by a 45 g semi-ellipsoid projectile at a velocity of around 2500 m/s yields the following conclusions.

1. Incorporating hook-ended steel fibers into concrete reduced the crater diameter and propagation of cracks. It also localized the damage by reducing the brittleness of concrete, and minimized the damage at both the front and the rear faces of the concrete slab. The crater and the cavity diameters in the rear face of a 2% fiber slab were 78% and 57% of those of plain concrete, respectively.
2. Incorporating hook-ended steel fibers in concrete does not only increase resistance to visible damage around the penetration crater, but also considerably increases resistance by reducing the residual velocity of the projectile. The residual velocity of the projectile decreased as the fiber volume fraction increased. However, this relationship was not linear. The residual velocity of the projectile was 75% and 44% of plain concrete when the fiber volume fraction exceeded 0.5% and 1.5%, respectively.
3. The failure of plain a concrete slab under high-velocity impact was catastrophic: it shattered into pieces with brittle failure. Additionally, the craters were more symmetric and circular when the fiber volume fraction exceeded 1.5%; the craters had sharp edges and were asymmetrical when the fiber volume fraction was under 1.5%.
4. Experimental findings showed that incorporated hook-ended steel fiber into concrete base protective elements will acquire visible damage resistant when the fiber volume fraction exceeded 1.5%.

References

ACI Committee 544.1R-96 (1997), "Fiber reinforced concrete".

Almansa, E.M. and Canovas, M.F. (1999) "Behavior of normal and steel fiber-reinforced concrete under impact of small projectiles", *Cement Concrete Res.* **29**, 1807-1814.

Analysis Laboratory, Ballistic (1961), "The resistance of various metallic materials to perforation by steel fragments; empirical relationships for fragment residual velocity and residual weight", Project THOR Technical report No. 47, April.

Anderson, W.F., J. Watson, A., and Armstrong, P.J. (1984), "Fiber reinforced concretes for the protection of structures against high velocity impact", In: Morton J, editor. *Proceeding of the International Conference on*

Structural Impact and Crashworthiness, London: Imperical College, 687-695.
Dancygier, A.N. and Yankelevsky, D.Z. (1996), "High strength concrete response to hard projectile impact", *Int. J. Impact. Eng.*, **18**(6), 583-599.
Gao, J., Sun, W., and Morino, K. (1997), "Mechanical properties of steel fiber-reinforced, high-strength, lightweight concrete", *Cement Concrete Comp.*, **19**, 307-313.
Leppanen, J. (2005), "Experiments and numerical analysis of blast and fragment impacts on concrete", *Int. J. Impact. Eng.*, **31**, 843-860.
Lloyd, R.M. (1998), "Conventional warhead systems physics and engineering design", *Progress in Astronautics and Aeronautics*, 179.
Luccioni, B.M. and Luege, M. (2006), "Concrete pavement slab under blast loads", *Int. J. Impact. Eng.*, **32**, 1248-1266.
Luo, Xin, Sun, Wei and Chan, Y.N. (2000), "Characteristics of high-performance steel fiber-reinforced concrete subject to high velocity impact", *Cement Concrete Res.*, **30**, 907-914,
Mindess, S., Bentur, A., Yan, C., and Vondran, G. (1989), "Impact resistance of concrete containing both conventional steel reinforcement and fibrillated polypropylene fibers", *ACI Mater. J.*, **86**(6), 545-549.
Ray, I., Chakraborty, A.K., and Sengupta, B. (2006), "High-performance concrete for containment structures", *Nucl. Eng. Des.*, **236**, 1041-1048.
Wafa, F.F. and Ashour, S.A. (1992), "Mechanical properties of high-strength fiber reinforced concrete", *ACI Mater. J.*, **89**(5), 449-455.
Walters, W.P. and Zukas, J.A. (1989), "Fundamentals of shaped charges", John Wiely and Sons, New York.
Zhang, M.H., Shim, V.P.W., Lu, G., and Chew, C.W. (2005), "Resistance of high-strength concrete to projectile impact", *Int. J. Impact. Eng.*, **31**, 825-841.
Zukas, J.A. and Walters, W. P. (1998), "Explosive effects and applications", Springer-Verlag New York, Inc.

CC